JOURNAL OF VIROLOGY, Dec. 2003, p. 13136–13145 Vol. 77, No. 24
0022-538X/03/$08.00+0 DOI: 10.1128/JVI.77.24.13136–13145.2003

Chromosomal Integration and Homologous Gene Targeting by Replication-Incompetent Vectors Based on the Autonomous Parvovirus Minute Virus of Mice

Paul C. Hendrie, Roli K. Hirata, and David W. Russell*

Department of Medicine, Division of Hematology, University of Washington, Seattle, Washington 98195

Received 15 May 2003/Accepted 4 September 2003

The molecular mechanisms responsible for random integration and gene targeting by recombinant adeno-associated virus (AAV) vectors are largely unknown, and whether vectors derived from autonomous parvoviruses transduce cells by similar pathways has not been investigated. In this report, we constructed vectors based on the autonomous parvovirus minute virus of mice (MVM) that were designed to introduce a neomycin resistance expression cassette (*neo*) into the X-linked human hypoxanthine phosphoribosyl transferase (*HPRT*) locus. High-titer, replication-incompetent MVM vector stocks were generated with a two-plasmid transfection system that preserved the wild-type characteristic of packaging only one DNA strand. Vectors with inserts in the forward or reverse orientations packaged noncoding or coding strands, respectively. In human HT-1080 cells, MVM vector random integration frequencies (*neo*$^+$ colonies) were comparable to those obtained with AAV vectors, and no difference was observed for noncoding and coding strands. *HPRT* gene-targeting frequencies (*HPRT* mutant colonies) were lower with MVM vectors, and the noncoding strand frequency was threefold greater than that of the coding strand. Random integration and gene-targeting events were confirmed by Southern blot analysis of G418- and 6-thioguanine (6TG)-resistant clones. In separate experiments, correction of an alkaline phosphatase (AP) gene by gene targeting was nine times more effective with a coding strand vector. The data suggest that single-stranded parvoviral vector genomes are substrates for gene targeting and possibly for random integration as well.

The *Parvoviridae* are nonenveloped viruses with an encapsidated, single-stranded, linear DNA genome of approximately 5 kb (3). Autonomous parvoviruses such as minute virus of mouse (MVM) are a diverse subgroup that differs from dependoviruses such as adeno-associated virus (AAV) in their ability to productively infect host cells in the absence of additional helper viruses (9). Unlike AAV, autonomous parvoviruses have not been shown to integrate into host chromosomes. Viral genomes were not detected in high-molecular-weight DNA during a lytic MVM infection (44) or in cells persistently infected with the immunosuppressive strain of MVM (45). Corsini et al. demonstrated that wild-type MVM can integrate into an episome containing the left terminal origin of replication in a reaction that depended on the viral nonstructural (NS) protein NS1 (7, 8). This reaction is analogous to AAV integration at viral repeat sequences that bind the AAV Rep proteins (33, 52). While Rep-dependent site-specific integration of AAV can occur at a sequence in human chromosome 19 similar to the viral terminal repeats (32, 49), murine and human genomes do not contain sequences homologous to the MVM binding and nicking sites for NS1 (see Materials and Methods), which may account for the lack of detectable MVM integration.

AAV vectors have been extensively developed for gene transfer applications (reviewed in references 6, 18, and 47) and are currently employed in clinical trails (1, 20, 29). In these applications, transduction can occur by gene addition from episomal and/or integrated vector genomes. Episomal expression requires the conversion of single-stranded vector genomes to double-stranded molecules either by annealing of complementary strands or second-strand synthesis (15, 17, 40). Vector integration (in the absence of Rep) occurs at random locations by nonhomologous recombination between terminally deleted vector genomes and host chromosomes (36, 39, 48, 53). A third means of transduction by AAV vectors is gene targeting with vectors containing sequences homologous to host chromosomes (46). The precise molecular events involved in random integration and gene targeting with AAV vectors are poorly understood. Specifically, it is not known whether the vector substrate is single stranded or double stranded, what the molecular structure of the host chromosome site is, and what host proteins are involved. A better understanding of these molecular events may lead to improvements in parvoviral vectors for gene therapy applications.

Vectors based on the autonomous parvoviruses have also been developed, with the hope of capitalizing on the oncotropic and oncolytic properties of the wild-type viruses for cancer therapy (12, 22, 37, 41). These vectors expressed the viral replication protein NS1, so transgene expression was assumed to occur from episomal vector genomes. Unlike AAV vectors, autonomous parvoviral vectors have not yet been shown to transduce cells by random chromosomal integration or gene targeting. Because these transduction pathways require only host enzymes, we reasoned that autonomous parvoviral vectors might behave the same as AAV vectors in these processes. In this report, we investigate integration and gene targeting with MVM vectors that retain only the terminal sequences necessary for replication and packaging. As with most

* Corresponding author. Mailing address: University of Washington, Department of Medicine, Mail Stop 357720, Seattle, WA 98195. Phone: (206) 616-4562. Fax: (206) 616-8298. E-mail: drussell@u.washington.edu.

AAV vectors, the viral replication proteins are not expressed from these MVM vector genomes so episomal replication should not occur. We also took advantage of the ability of MVM to package predominantly the minus strand of the viral genome (5, 10) to prepare vectors that contain either the coding or noncoding strand of the transgene cassette. In the case of AAV, similar amounts of both strands are packaged (4). This allowed us to investigate the relative efficiencies of coding and noncoding strands, alone and in combination, for random integration and gene targeting.

MATERIALS AND METHODS

Cell culture. HT-1080 (43), HT/LAP375Δ4SPc9, 293T (11), and NB324K cells (51), a gift from Peter Tattersall, were cultured in Dulbecco's modified Eagle medium (DMEM) with 10% heat-inactivated fetal bovine serum (HyClone), penicillin (100 U/ml), and streptomycin (100 μg/ml) at 37°C in a 5% CO_2 atmosphere. Prior to transduction in *HPRT* experiments, HT-1080 cells were cultured in HAT medium (DMEM containing 13.61-μg/ml hypoxanthine, 0.176-μg/ml aminopterin, and 3.875-μg/ml thymidine) to select against cells containing mutations in the *HPRT* gene.

Plasmids. The infectious clone of MVM, pMVMp (19), was a gift from Peter Tattersall. The packaging plasmid pPMp was made by inserting a *Pme*I-*Sna*BI restriction fragment from pMVMp (nucleotides 133 to 4631; GenBank accession no. J02275) with attached *Bam*HI linkers into pVZ1 (23). The vector plasmid pMB was made by deleting the *Pme*I-*Xba*I restriction fragment from pMVMp (nucleotides 133 to 4342; GenBank accession no. J02275), attaching *Bgl*II linkers, and religating. To insert an MVM NS1 binding and nick site 5′ to the left terminal palindrome of pMB, the oligonucleotides 5′-GATCCTTCGAAACTC CCTGAACCGCTTATCATTTTTAGAACTGACCAACCATGTTCAC-3′ and 5′-GTGAACATGGTTGGTCAGTTCTAAAAATGATAAGCGGTTCAGGG AGTTTCGAAG-3′ were hybridized and used to replace the *Bam*HI-*Bsa*AI fragment at the left-terminal palindrome of pMB via subcloned intermediates to create pMNB. Vector plasmids pMHPe3TNA-f and pMHPe3TNA-r were made by inserting an *Ecl*136II-*Bgl*II fragment from pA2HPe3TNA (24) into the *Bgl*II site of pMNB in opposite orientations. pMHPe3TNA-f, pMHPe3TNA-r, and pA2HPe3TNA all contain the same *HPRT-neo* cassette consisting of nucleotides 14895 to 17809 of the human *HPRT* locus (GenBank accession code HUMHPRTB) with the 1.14-kb *Xho*I-*Sal*I fragment of pMC1neoPolyA (Stragagene, La Jolla, Calif.) inserted at the *Xho*I site of exon 3 in *HPRT*.

MVM vector plasmids pM5′APMscvF-f and pM5′APMscvF-r were made by inserting a 3,498-bp *Bgl*II fragment containing the 5′ portion of the human placental alkaline phosphatase (AP) gene from pA2-5′APBss (25) into the *Bgl*II site of pMNB (see Fig. 8) in the forward and reverse orientations, respectively. Both plasmids also contained a 1,186-bp *Bam*HI-*Bst*Z17I fragment from pCGPMscvF (28) that included a green fluorescent protein (GFP) gene driven by the mouse stem cell virus long terminal repeat (LTR) promoter (Mscv). The GFP gene uses the MVM polyadenylation signals retained in pMNB.

Retroviral vector plasmid pLAP375Δ4SP is derived from pLAP375Δ4SN, which contains an AP gene with a 4-bp deletion at nucleotide 375 of the AP reading frame (25). The puromycin *N*-acetyltransferase (*puro*) gene (nucleotides 182 to 906; GenBank accession no. M25346) in pLAP375Δ4SP replaces the *neo* gene in pLAP375Δ4SN.

Vector and virus production. AAV vector stocks were made as previously described (24) by transient cotransfection of 293T cells with pA2HPe3TNA and serotype 2 helper plasmid pDG (21). MVM vector stocks were prepared by transient cotransfection of 293T cells (30 10-cm-diameter dishes seeded at 10^6 cells per dish the day before) with pPMp (16 μg/dish) and MVM vector plasmids (4 μg/dish). Cells were harvested 3 days posttransfection with a rubber policeman, collected into 50-ml centrifuge tubes, pelleted by centrifugation (390 × *g*, 5 min, 20°C), resuspended in lysis buffer (0.15 M NaCl, 50 mM Tris [pH 8.5]), frozen and thawed three times, and incubated with benzonase (EM Industries [final concentration greater than 50 U/ml]) 30 min at 37°C, and then cellular debris was pelleted by centrifugation (Sorvall HS4 rotor, 4,100 × *g*, 30 min, 4°C). For iodixanol gradients, the resulting suspension was first adjusted to 1 M NaCl and then mixed with OptiPrep (Nycomed Pharma Centrifugation Media) to a final iodixanol concentration of 36% (wt/vol) and centrifuged (Beckman NVT65 rotor, 290,000 × *g*, 3 h, 4°C). Starting from the gradient bottom, 0.5-ml (fractions 1 to 10) or 1.0-ml (fractions 11 to 15) fractions were collected with an 18-gauge needle. For each fraction, the density (ρ) was determined from the refractive index (RI) obtained by using a refractometer (Milton Roy Company) and the equation ρ = [(3.242 × RI) − 3.323] g/ml. The full-length genome content of each fraction was determined by alkaline Southern blot analysis as described previously (27). The fractions with the highest genome content were pooled and concentrated with an Ultrafree-15 centrifugal filter device (Millipore) to a final volume of 1 ml in DMEM. AAV and MVM vector particle titers were based on the number of full-length, single-stranded DNA genomes detected by alkaline Southern blot analysis (27). Wild-type MVM stocks were made in a similar fashion, except plasmid pMVMp was used for the transfections (20 μg/10-cm dish), and an NS-specific *Bsm*BI fragment probe (MVMp nucleotides 229 to 928; GenBank accession no. J02275) was used for quantitation. Retroviral vector stocks were made with pLAP375Δ4SP as described previously (25).

Transduction assays. Transduction experiments with *HPRT* vectors were performed as previously described for AAV vectors (24), by plating 2×10^4 HT-1080 cells into 48-well plates on day 1, infecting with vector stocks on day 2, treating with trypsin and replating in 10-cm dishes on day 3, and then expanding in nonselective medium for 9 days to allow for loss of existing HPRT protein. After this phenotypic expression period, cells were plated at different dilutions in DMEM containing G418 (0.7-mg/ml active compound), 6-thioguanine (6TG; 5 μg/ml), or no selective agent to determine plating efficiency. Colonies were stained with Coomassie blue and counted after 8 days of growth. Transduction frequencies were determined by dividing the number of G418- or 6TG-resistant colonies obtained by the number of unselected colonies obtained.

For AP experiments, HT-1080 cells were first transduced with pLAP375Δ4SP-derived retroviral vector stocks as previously described (25), followed by selection with puromycin (final concentration, 0.6 mg/ml). A single clone (HT/LAP375Δ4SPc9) was isolated, shown to have a single integrated retroviral provirus by Southern blot analysis, and used for gene-targeting experiments. To detect AP gene correction, 2×10^4 HT/LAP375Δ4SPc9 cells were plated into 48-well plates on day 1, infected with vector stocks on day 2, treated with trypsin on day 3, and split into three dishes. One 6-cm dish received 0.2% of the infected cells and was stained 1 day later to determine the number of viable cells per well. Another 6-cm dish received 49.8% of the infected cells, was cultured for 3 days, and then used to determine the percentage of GFP-expressing cells by flow cytometry (FACscan; Becton Dickinson). A third dish (10 cm) received 50% of the infected cells, was cultured for 7 days, and then was stained for AP expression as previously described (16). The number of AP^+ foci per 10^5 plated cells was determined by dividing the number of AP^+ foci obtained by the number of viable cells plated in that dish and multiplying the quotient by 10^5 as described previously (25).

Two-tailed Student's *t* tests were used to determine significant differences among transduction frequencies.

DNA analysis. 6TG- and G418-resistant colonies were isolated with cloning rings and expanded, and genomic DNA was extracted with the Puregene kit (Gentra). To prepare episomal Hirt supernatant DNAs, 4×10^4 HT-1080 cells were infected with 2×10^9 genome-containing particles of MVM-HPe3TNA-f, the cells were harvested with rubber policemen into ice-cold phosphate-buffered saline (PBS) with 1.0 mM EDTA at various times after infection, rinsed, and pelleted (16,000 × *g*, 35 s, 20°C), and DNA was isolated by a modified version of the method described by Hirt (26). Cell pellets were resuspended in 10 mM Tris (pH 7.4)–10 mM EDTA (approximately 235 μl/10^6 cells), and sodium dodecyl sulfate (SDS) was added to a final concentration of 0.6%. After a 20-min incubation at 20°C, 5 M NaCl was added to a final concentration of 1 M, and the samples were incubated at 4°C overnight and then centrifuged at 16,000 × *g* for 30 min at 4°C. The supernatants were treated with 1 μl of proteinase K (20 mg/ml) for 1 h at 37°C, extracted twice with phenol-chloroform and once with chloroform, and precipitated with ethanol. Pellets were resuspended in 20 μl of 10 mM Tris (pH 8.0)–1 mM EDTA. Southern blots were performed by standard techniques with random-primed double-stranded probes prepared with Rediprime II (Amersham Biosystems) or single-stranded probes created with the Riboprobe in vitro transcription system (Promega). Quantitation of Southern blots was performed by PhosphorImager analysis (Molecular Dynamics).

Replication center assay. Stocks were tested for replication-competent MVM (RCV) by a single-cycle replication center assay using the permissive cell line NB324K. A total of 5×10^3 cells were seeded in 96-well plates, infected with dilutions of vector stock or wild-type MVM 24 h later, harvested with trypsin 48 h after infection, and then transferred to nylon membranes and lysed as previously described for AAV (31). Replication centers were detected with a 5′ NS probe (nucleotides 223 to 921, GenBank accession no. J02275) and visualized as radioactive spots on autoradiographs.

Murine and human genome database search. A nucleotide BLAST search was performed with the National Center for Biotechnology Information web site (www.ncbi.nlm.nih.gov) to search the murine and human genomes for the MVM sequences CTTATCATTTTTAGAACTGACCAAC and CTATTCAGTGAAC

CAAC, which contain the binding and nicking sites for MVM NS1 from the 3′ and 5′ ends of the MVM genome.

RESULTS

Replication-incompetent MVM vector production. A two-plasmid vector production system was developed based on the cloned infectious genome of the prototypic wild-type strain of MVM (35). The packaging plasmid pPMp contains the viral genes and provides the viral proteins in *trans*, but lacks the terminal palindromes required for replication and packaging (Fig. 1A). The vector plasmid backbone pMNB contains the *cis*-acting terminal palindromes, but lacks the viral promoters and most of the viral open reading frames. The vector backbone retains the 3′ portion of the VP1 and VP2 genes required for efficient replication (50), and a nicking site for the NS1 protein was introduced outside the left-terminal palindrome to improve production of recombinant viral vectors (30). A unique *Bgl*II site can be used to introduce nonviral DNA into the pMNB backbone.

We created vectors that could simultaneously transduce cells either by chromosomal integration of a selectable neomycin resistance gene (*neo*) or by homologous gene targeting and disruption of the X-linked human *HPRT* gene. These vectors contain 2,915 bp of genomic *HPRT* sequence with a *neo* gene under the control of the herpes simplex virus thymidine kinase (TK) promoter inserted in exon 3 of *HPRT* (Fig. 1B). Vectors MVM-HPe3TNA-f (forward orientation) and MVM-HPe3TNA-r (reverse orientation) contain the same *HPRT* and *neo* sequences in opposite orientations relative to the terminal palindromes, and they should lead to packaging of the noncoding and coding strands of these genes, respectively. The AAV control vector AAV-HPe3TNA (24) contains the identical *HPRT-neo* cassette, but should package both strands in similar quantities. Transduced cells containing either randomly integrated vector genomes or targeted *HPRT* alleles should be resistant to G418, and diploid male cells with targeted *HPRT* alleles should be *HPRT* negative and resistant to 6TG.

MVM vector stocks were made by cotransfection of 293T cells with vector and packaging plasmids, harvesting of cell lysates 3 days later, and purification on an iodixanol density gradient. The full-length vector genome content of each gradient fraction was quantified by alkaline Southern blot analysis (Fig. 2A). The majority of the full-length genomes banded at 50 to 60% (wt/vol) iodixanol, corresponding to a density of approximately 1.3 g/ml. Fractions containing the vector genomes were pooled and concentrated, which typically resulted in stocks containing over 10^{11} genome-containing vector particles in 1 ml. Forward (MVM-HPe3TNA-f) and reverse (MVM-HPe3TNA-r) vector stocks were compared by Southern blot analysis for their content of coding and noncoding strands by using sense and antisense RNA probes (Fig. 2B). As predicted, the forward and reverse vector stocks contained noncoding and coding strands, respectively, by this assay, with no detectable signal from the complementary strands (less than ~5% of the total signal).

Random integration of MVM vectors. HT-1080 cells, a human male osteosarcoma cell line, were infected with vector MVM-HPe3TNA-f and/or MVM-HPe3TNA-r, passaged for 9 days in nonselective medium to allow for loss of preexisting HPRT protein and expression of the *neo* gene, and then plated in G418 to select for cells with an integrated *neo* cassette (Fig. 3, open bars). The percentage of G418-resistant cells ranged from 3 to 5% for the forward orientation vector, reverse orientation vector, or the vector mixture (open bars, Fig. 3). As a

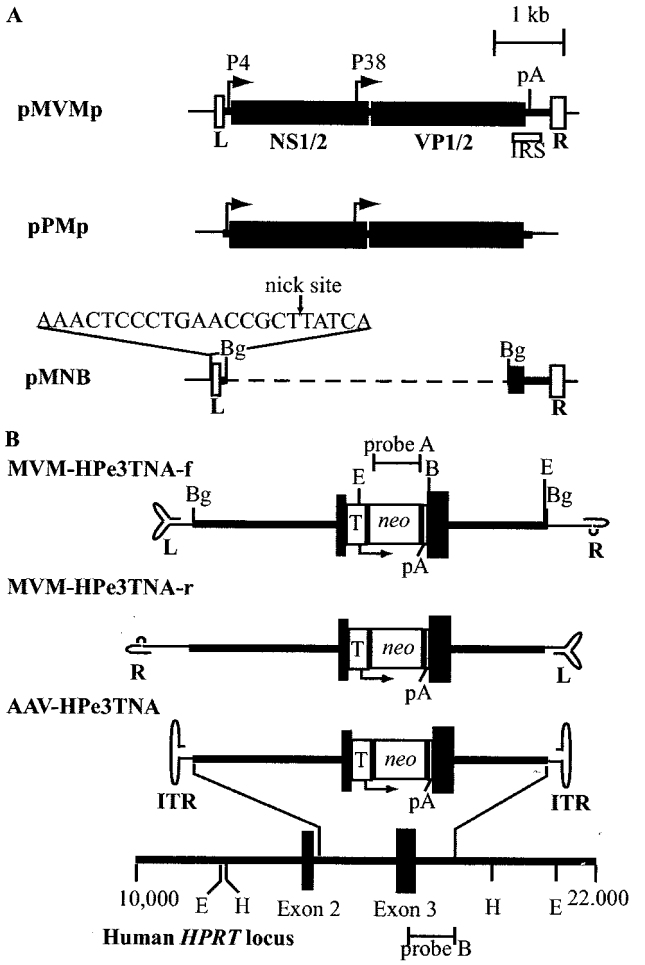

FIG. 1. Plasmids and vectors used in this study. (A) Maps of wild-type MVM plasmid pMVMp, packaging plasmid pPMp, and vector backbone plasmid pMNB are shown. The left (L)- and right (R)-terminal palindromes are indicated by open boxes. Solid boxes represent the viral open reading frames for the nonstructural proteins (NS1/2) and capsid proteins (VP1/2). The MVM P4 and P38 promoters are shown with arrows. The location of the first polyadenylation (pA) signal is shown. The location of the *cis*-acting internal replication sequence (IRS) is shown by an open box below pMVMp. The viral sequence is shown as a thick line. The dashed line represents deleted viral sequence. The sequence of the inserted NS1 nick site is shown above pMNB. (B) Maps of MVM and AAV targeting vectors and the human *HPRT* locus are shown. Locations the of *HPRT* exons (black boxes), introns (thick lines), AAV inverted terminal repeats (ITR), MVM left (L)- and right (R)-terminal palindrome sequences, TK promoter (T), *neo* gene, pA sites, and the *neo* and *HPRT* hybridization probes used (probes A and B, respectively) are shown. The AAV and MVM vector terminal repeats are shown in their base-paired secondary structures. Each vector contains the same 4,073-bp targeting cassette composed of 2,915 bp of the *HPRT* locus sequence with the *neo* expression cassette disrupting the centrally located exon 3. Relevant endonuclease restriction sites (*Bam*HI, B; *Bgl*II, Bg; *Eco*RI, E; *Hin*dIII, H) are shown in panels A and B.

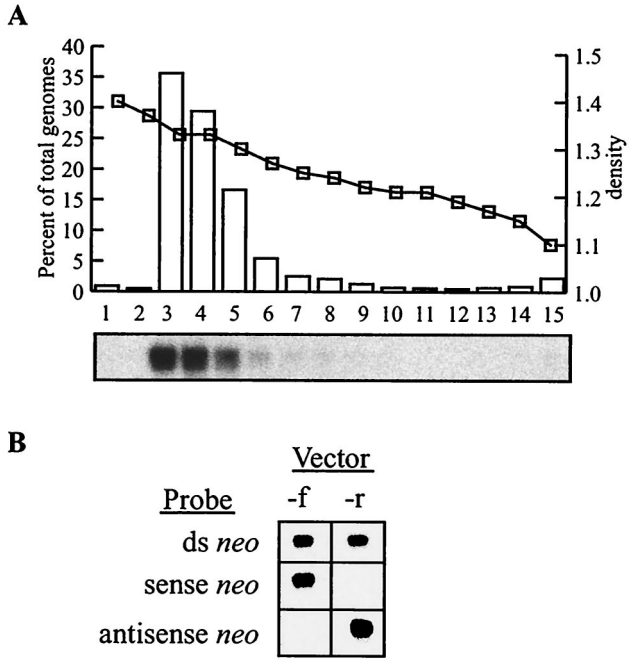

FIG. 2. Characterization of MVM vector stocks. (A) Vector MVM-HPe3TNA-f was purified on an iodixanol gradient, and 2 μl of each fraction was analyzed on an alkaline Southern blot probed for *HPRT* sequences. The graph depicts the percentage of total genomes present in each fraction (bars) determined by PhosphorImager quantification of the Southern blot (autoradiograph shown below graph), and the calculated density (squares) determined from the RI of each fraction. (B) Strand-specific alkaline Southern blot analysis of MVM-HPe3TNA-f (forward) and MVM-HPe3TNA-r (reverse) vector stocks (3×10^8 genomes each) hybridized with a double-stranded *neo* probe (top row), a T7 sense *neo* transcript (middle row), or a T3 antisense *neo* transcript (bottom row).

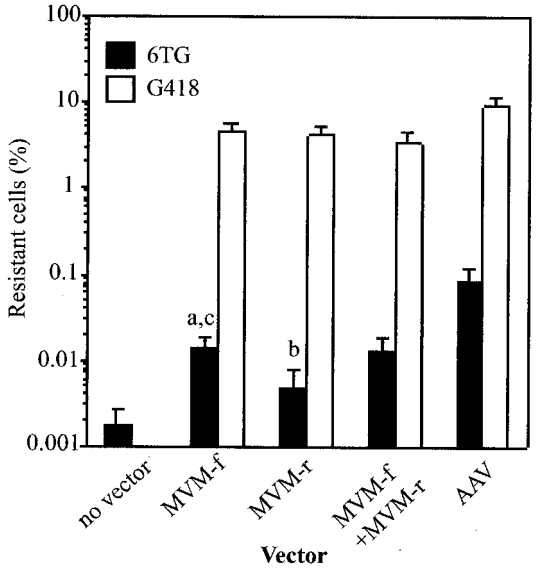

FIG. 3. Transduction frequencies of MVM and AAV vectors. A total of 4×10^4 HT-1080 cells were transduced with the indicated vector preparation (2×10^{10} particles of MVM-HPe3TNA-f [MVM-f] or MVM-HPe3TNA-r [MVM-r], 1×10^{10} particles of both MVM-f and MVM-r, or 2×10^9 particles of AAV-HPe3TNA [AAV]) and expanded for 10 days, and then the percentage of G418- or 6TG-resistant cells was determined by plating portions in G418, 6TG, or nonselective medium (see Materials and Methods). The G418 (open bars) and 6TG (solid bars) resistance frequencies were determined by dividing the number of G418- or 6TG-resistant colonies obtained by the number of unselected colonies obtained. The mean and standard deviation of five experiments (MVM vector infections) or four experiments (AAV infections) are shown. The *P* values for student *t* tests comparing 6TG resistance frequencies of MVM-f to those of the no-vector control (a), MVM-r versus control (b), and MVM-f versus MVM-r (c) were $P < 0.005$, $P = 0.069$, and $P = 0.015$, respectively.

comparison, the similar AAV vector transduced cells at slightly higher frequencies, but with one-tenth the multiplicity of infection (MOI).

We determined the molecular structure of 30 G418-resistant HT-1080 clones by Southern blot analysis: 10 each from cells treated with the forward vector, reverse vector, and the vector mixture (Table 1). Digests of four example clones are shown in Fig. 4. Integration was observed in all 30 clones based on the high-molecular-weight *neo*-hybridizing signal of uncut as compared to *Hin*dIII-digested genomic DNA. *Hin*dIII does not cut within the vector genome, so each vector band represents a different integration site. The *Hin*dIII vector fragments from different clones had distinct sizes, suggesting that integration occurred at random chromosomal locations. In 13 of 30 clones, we observed multiple integration sites, based on the presence of multiple vector bands after *Hin*dIII digestion (clone 3 in Fig. 4). The number of different integrations per clone ranged from 1 to 4 (Table 1) (data not shown). One clone from each infection type had multiple bands when digested with *Bam*HI (an endonuclease that cuts once within the vector), but a single *Hin*dIII vector band, as demonstrated by clone 4. This likely represents multiple vector genomes integrated at a single chromosome site as a concatemer. Since the vector DNA may not have integrated intact, we also digested with *Bgl*II, which cuts just inside each terminal palindrome of the vector to produce a 4.1-kb *Bgl*II insert. Only 9 of 30 clones had an intact 4.1-kb *Bgl*II vector band (clones 1 and 4 in Fig. 4), suggesting that in most cases the integrated vector provirus did not include the terminal sequences flanking at least one of the vector *Bgl*II sites.

Gene targeting at the human *HPRT* locus with MVM vectors. HT-1080 cells were infected with MVM-HPe3TNA-f and/or MVM-HPe3TNA-r, and *HPRT*-negative colonies were selected with 6TG (solid bars, Fig. 3). The *HPRT* gene-targeting frequency of the forward vector (0.015%) was three times greater than that of the reverse vector (0.0055%). Infection with an equal mixture of forward and reverse vectors did not significantly increase the targeting frequency compared to infection with the forward vector alone (0.014 versus 0.015%). The gene-targeting frequencies of MVM vectors were 2 to 3 logs lower than the gene addition frequencies measured in the same experiments as G418-resistant colonies, which were similar for each vector and served as internal controls for the biological activity of each vector preparation. In control experiments, the AAV targeting vector had fivefold-higher targeting frequencies than the MVM forward vector at one-tenth the MOI. In the cell population not infected with vectors, 0.0023% of cells were 6TG resistant, representing spontaneous mutations at *HPRT*.

TABLE 1. Analysis of genomic DNA from G418- and 6TG-resistant clones of HT-1080 infected with MVM vectors

Vector	G418 resistance[a]				6TG resistance			
	No. of integration sites/cell		4.1-kb *Bgl*II fragment	No. with concatemer	No. of clones analyzed	No. of expt.	No. (%) of clones	
	Single	Multiple					Targeted	Targeted + random
Forward	7	3	4	1	20	3	17 (85)	0 (0)
Reverse	4	6	3	1	12	3	10 (83)	7 (70)
Mixture	5	5	2	1	10	1	10 (100)	2 (20)

[a] 10 clones analyzed for each vector.

Southern blot analysis of genomic DNA from 6TG-resistant clones was performed to confirm that targeted insertion of the *neo* gene into exon 3 of the human *HPRT* locus had occurred. Five representative clones from cells treated with the forward vector, reverse vector, or the vector mixture are shown in Fig. 5. After digestion with *Hin*dIII or *Eco*RI, targeted loci were identified by the predicted shift in the *HPRT*-hybridizing band and confirmed by hybridization to a *neo* probe. Thirty-seven of 42 6TG-resistant clones (88%) from three independent experiments had the bands predicted for targeted loci (Table 1). The five clones that did not show targeted loci likely represented spontaneous mutations in *HPRT* that can also occur in the absence of infection with the vector. For example, forward clone 2 in Fig. 5 contained unexpected *Hin*dIII and *Eco*RI bands that hybridized to *HPRT*. Since the same fragments did not hybridize to the vector-specific *neo* probe, there is no evidence that the novel bands were due to the targeting vector. Similarly, reverse clone 5 in Fig. 5 deleted this region of *HPRT*, based on the lack of hybridizing bands. In some clones, additional *HPRT*- and *neo*-hybridizing bands were present, representing random vector integration events that also occurred in targeted clones (reverse clones 1 and 2 in Fig. 5). Interestingly, these additional random integration events were especially common in cells targeted with the reverse vector (7 of 10 targeted clones) compared to the forward vector (0 of 17 targeted clones). None of the 30 G418-resistant clones described above had a targeted *HPRT* allele (data not shown), consistent with the low frequency of gene targeting compared to random integration.

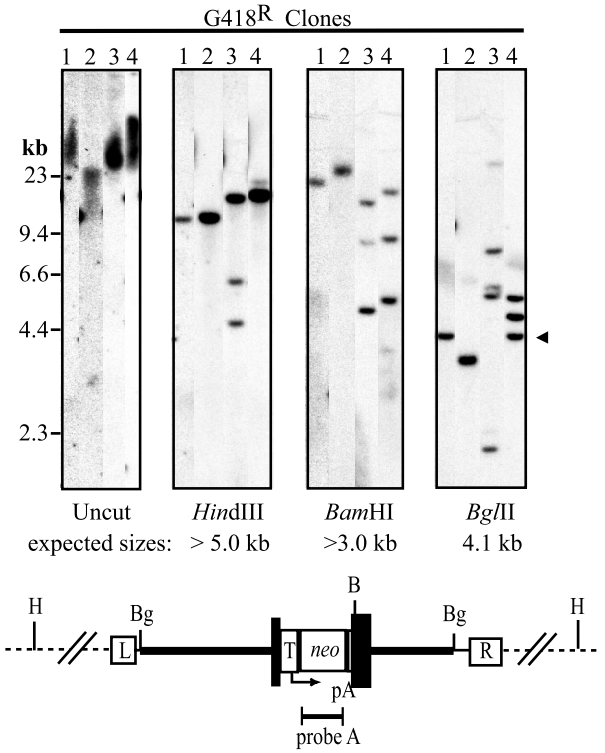

FIG. 4. Southern blot analysis of G418-resistant HT-1080 clones. Genomic DNAs from four representative G418-resistant clones were isolated on 1% agarose gels without digestion or after digestion with *Hin*dIII, *Bam*HI or *Bgl*II, and probed for *neo* sequences. The positions of size standards and the expected 4.1-kb *Bgl*II vector fragment are shown to the left and right of the panels, respectively. The predicted structure of an integrated provirus is shown below the panels with the locations of *HPRT* intron sequences (thick line), *HPRT* exon 3 (dark boxes), MVM right (R)- and left (L)-terminal palindromes, TK promoter (T), *neo* gene, pA sites, and relevant restriction sites (*Bam*HI, B; *Bgl*II, Bg; *Hin*dIII, H) indicated.

Transduction by MVM vectors does not require viral proteins. Recombinant infectious particles were sometimes generated during transfection of MVM vector and packaging plasmids as described previously (13). Although our stocks did not contain infectious MVM based on the lack of cytopathic effects produced (data not shown), recombination during vector production could still have led to packaging of noninfectious particles containing viral genes. If the NS1 gene had been packaged, these contaminating particles would have been competent for DNA replication, which may have affected the transduction process. We performed replication center assays to determine the presence of RCV in our vector stocks. Permissive NB324K cells were exposed to dilutions of vector stocks, cultured for 2 days, transferred to nylon membranes, and then probed for the presence of amplified NS1 sequences not present in the vector. Individual cells infected with RCV form radioactive spots on the nylon membrane. By this assay, we could not detect RCV in four of four stocks, with a sensitivity of less than 1 RCV per 10^8 vector genomes (Fig. 6). As a positive control, we detected 43 RCV per 10^5 genome-containing particles of a wild-type MVM stock. Therefore, 1 RCV represents ~2,300 NS1-containing wild-type particles in this assay (10^5/43), so our vector stocks contained less than 2,300 NS1-containing particles per 10^8 vector genome-containing particles. This result is likely due to our vectors having limited 3′ homology (289 bp) and no 5′ homology with the packaging plasmid pPMp. In transduction experiments, we infected 4×10^4 HT-1080 cells with 2×10^{10} MVM vector particles, so there was less than 0.005 RCV per cell (200 RCV/40,000 cells),

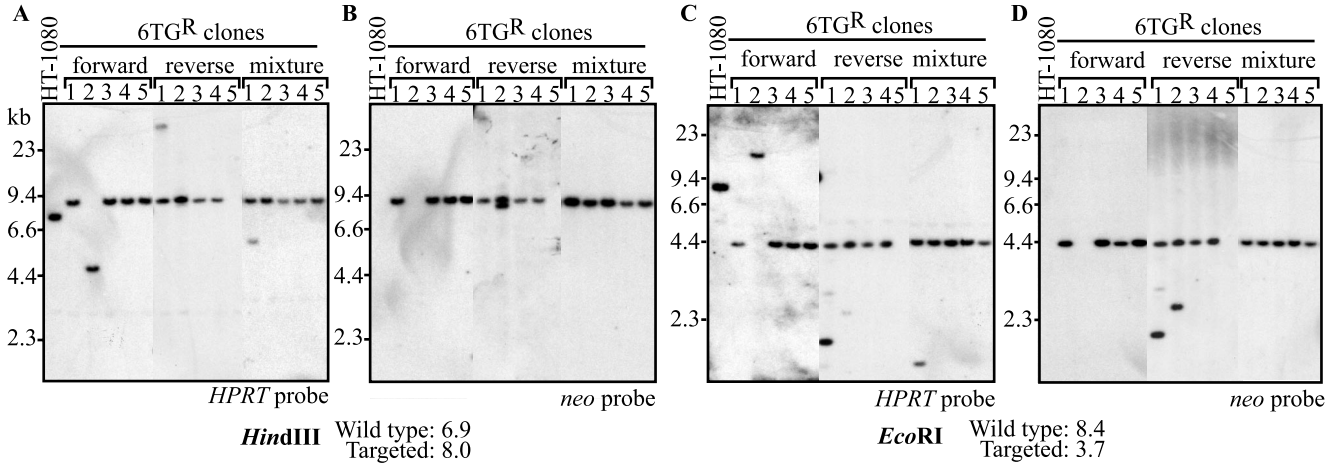

FIG. 5. Southern blot analysis of 6TG-resistant HT-1080 clones. Genomic DNAs from 15 6TG-resistant clones (5 each from cells transduced with MVM-HPe3TNA-f, MVM-HPe3TNA-r, and the mixture of vectors) and untransduced, parental HT-1080 cells were digested with *Hin*dIII (A and B) or *Eco*RI (C and D) and probed for *HPRT* (A and C) or *neo* (B and D) sequences. The positions of size standards are shown to the left of each panel, and the predicted fragment sizes of wild-type and targeted alleles are indicated. The locations of restriction sites and the probe fragments are shown in Fig. 1.

making it unlikely that RCV and, in particular, NS1 expression affected transduction frequencies.

To further demonstrate that viral gene expression was not required for transduction by MVM vectors, we included wild-type MVM during the transduction period (Table 2). The addition of wild-type MVM at an MOI of 2.5 RCV per cell (5.8×10^3 genome-containing particles per cell and 500 times the maximum possible contamination level of our stocks) did not significantly change the random integration frequencies for the forward or reverse vectors as measured by G418 resistance. Similarly, wild-type MVM did not significantly increase the *HPRT* targeting frequencies for the forward vector as measured by 6TG resistance. With the reverse vector, there was a trend for higher targeting frequencies in the presence of wild-type MVM that may relate to the overall lower targeting frequencies of this vector (see Table 1), but it did not reach statistical significance.

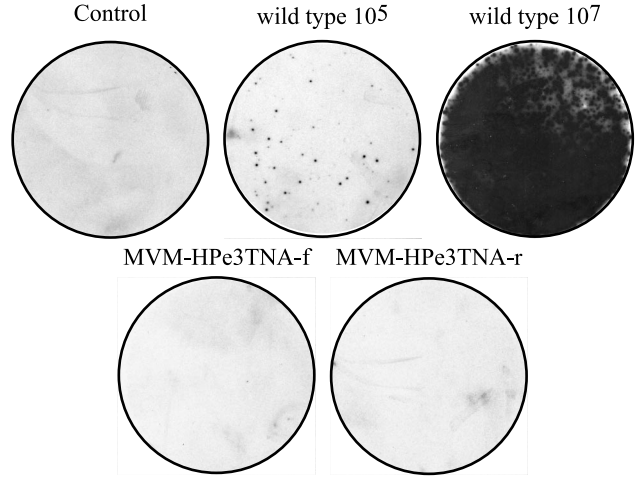

FIG. 6. Replication center assay. NB324K cells were left uninfected (control) or were infected with the indicated amounts of genome-containing particles of wild-type MVM and 10^8 MVM vector genomes, cultured for 2 days, aspirated onto nylon membrane filters, lysed, and then hybridized to a 5′ NS1 probe. Radioactive spots represent individual cells with replicated NS1-containing genomes due to infection with RCV.

Most intracellular MVM vector genomes remain single stranded. Since the wild-type MVM genome is converted by second-strand synthesis to a double-stranded intermediate as the first step of viral replication, we isolated episomal Hirt supernatant DNA (26) from infected cells to determine whether intracellular vector genomes were single or double stranded. Second-strand synthesis occurs by extension from the left-terminal palindrome (5), so the resulting double-stranded molecule is covalently linked at the left terminus and should migrate as a dimer-size molecule on a denaturing alkaline gel. We could not detect dimer (d) vector genomes in Hirt supernatants at any time after infection (Fig. 7A; sensitivity 0.04% of input vector genomes). Furthermore, the nonpackaged, coding strand was not present based on probing with antisense transcripts (Fig. 7B; sensitivity 0.02% of input vector genomes). Thus, while we cannot rule out that rare double-stranded vec-

TABLE 2. Effect of wild-type MVM on transduction of HT-1080 cells[a]

Vector	Wild-type MVM	% of resistance in expt.						Avg % ± SD[b]
		G418			6TG			
		1	2	3	1	2	3	
None	−	0	0	0	0.0027	0.0015	<0.0008	
None	+	0	0	0	0.0018	<0.0004	<0.007	
Forward	−	6.0	3.6	ND[c]	0.013	0.012	ND	
Forward	+	3.2	3.4	ND	0.012	0.013	ND	
Reverse	−	4.8	2.7	1.7	0.0066	0.0035	0.0014	0.0034 ± 0.0023
Reverse	+	2.8	2.7	2.5	0.015	0.0092	0.0042	0.0095 ± 0.0054

[a] In three separate experiments, wild-type MVM (MOI, 2.5 RCV per cell) was added alone or in combination with the indicated MVM-HPe3TNA vector stock (MOI of 5×10^5 genome-containing particles per cell). The percentage of G418- and 6TG-resistant cells was determined as described in Materials and Methods.
[b] Average values ± standard deviations (SD) are shown for the reverse vector.
[c] ND, not determined.

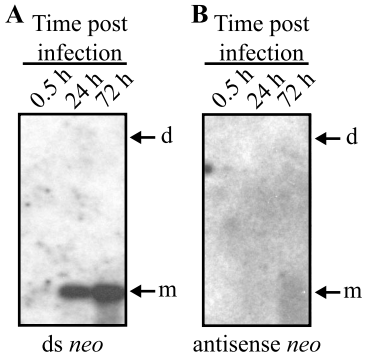

FIG. 7. Determination of the intracellular form of MVM vector genomes. Shown are the results of Southern blot analysis of Hirt supernatants from 4×10^4 HT-1080 cells infected with 2×10^9 genome-containing particles of MVM-HPe3TNA-f prepared 0.5, 24, and 72 h after infection. One-fourth of each sample was run on 0.8% alkaline agarose gels, transferred to nylon membranes, and hybridized with a double-stranded *neo* probe (A) or a single-stranded antisense *neo* probe (B). Arrows to the right of each panel show expected locations of single-stranded monomer (m) and dimer (d) genomes.

tor episomes participate in the transduction process, there is no evidence for second-strand synthesis of entering MVM vector genomes or for delivery of complementary strands. In comparison to purified vector stock DNA, the amounts of monomer (m) genomes detected in Hirt supernatants were 1.3 and 3.1% of the total input inoculum 24 and 72 h after infection, respectively, with smaller amounts present 0.5 h after infection.

Comparison of coding and noncoding MVM vector strands in a second gene-targeting system. As described above, *HPRT* gene-targeting frequencies were significantly higher with the noncoding strand vector as opposed to the coding strand vector. To address whether this strand preference was unique to the *HPRT* system, we constructed MVM vectors that can correct a mutant alkaline phosphatase gene. In this system (25), an integrated copy of a mutant AP gene is introduced by a retroviral vector (LAP375Δ4SP), then corrected by gene targeting with a parvoviral vector (Fig. 8A). Cell line HT/LAP375Δ4SPc9 is a clone of HT-1080 cells containing a single AP target site (see Materials and Methods). Vectors MVM-

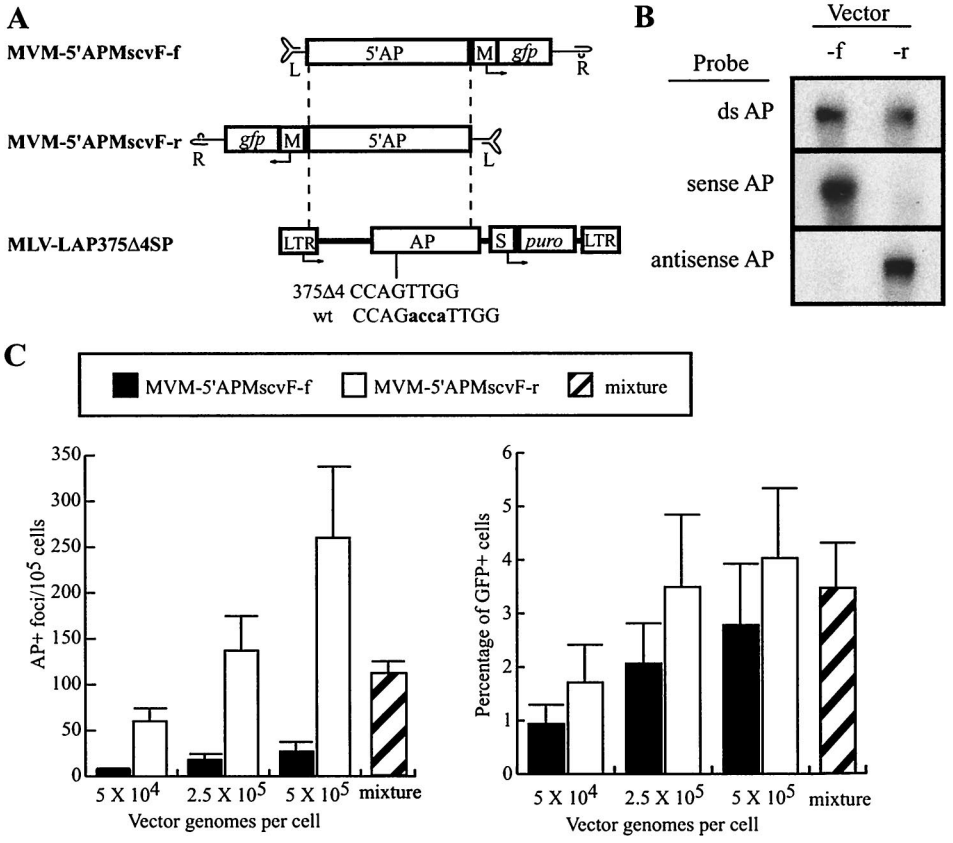

FIG. 8. AP gene-targeting experiments. (A) Diagrams of MVM and retroviral vectors for AP gene targeting are shown. The murine leukemia virus (MLV) retroviral vector LAP375Δ4SP is shown with the positions of the LTR, AP gene, SV40 promoter (S), and puromycin resistance gene (*puro*) indicated. The 4-bp deletion in AP is shown below the AP gene along with the corresponding wild-type (wt) sequence: the deleted bases are lowercase and boldface. Maps of MVM targeting vectors containing 5′ portions of the AP gene are shown above the MLV-LAP375Δ4SP target site, with the locations of left (L)- and right (R)-terminal palindrome sequences, murine stem cell virus LTR promoter (M), and green fluorescent protein (*gfp*) indicated. Each targeting vector contains 2,498 bp of homology to the target sequence, as indicated by dashed lines. (B) Strand-specific alkaline Southern blot analysis of MVM-5′APMscvF-f (forward) and MVM-5′APMscvF-r (reverse) vector stocks (1×10^9 genomes each) hybridized with a double-stranded AP probe (top row), a T7 sense AP transcript (middle row), or a T3 antisense AP transcript (bottom row). (C) AP gene-targeting rates and GFP gene addition rates are shown for MVM-5′APMscvF-f (solid bars), MVM-5′APMscvF-r (open bars), and a mixture of both vectors (hatched bars) in HT/LAP375Δ4SPc9 cells at the indicated MOIs. The mixture contained 2.5×10^5 genomes of forward and reverse vector stocks. Mean values are shown with standard deviations from three independent experiments.

5′APMscvF-f and MVM-5′APMscvF-r contain the 5′ portion of the AP open reading frame in the forward and reverse orientations, respectively, as well as a GFP expression cassette that served as an independent measure of transduction. Strand-specific packaging of these MVM vector stocks is shown in Fig. 8B, with the forward (f) and reverse (r) vector stocks packaging >94% noncoding strands and >97% coding strands, respectively. Both vectors corrected the AP mutation by gene targeting in a dose-dependent manner, and at each MOI, the reverse vector performed significantly better ($P < 0.05$) than the forward vector (frequency of 7.6 to 9.6 times higher). Both vectors also produced GFP-positive cells in a dose-dependent manner by gene addition, and although the reverse vector performed slightly better (frequency of 1.4 to 1.8 times higher), this difference did not reach statistical significance ($P > 0.1$). Transduction by a mixture of equal quantities of forward and reverse vectors (2.5×10^5 genomes each) was not statistically different from that with the reverse vector alone (2.5×10^5 genomes). Thus, as with *HPRT* vectors, the MVM AP vectors demonstrated a clear strand bias for gene targeting, but not for gene addition.

DISCUSSION

In this report, we have developed a system for the production of MVM vectors lacking all viral genes. The MVM vectors described previously expressed NS1 (2, 12–14, 30, 42), which allowed them to replicate in permissive cell types. A vector based on the autonomous parvovirus LuIII that lacked all viral proteins has been described, but there was no DNA analysis, and it was assumed that the transient transduction observed was due to episomal expression (34). Our vectors contained no NS sequences and only a small 3′ portion of VP sequence, so they are replication incompetent. The two-plasmid transient transfection system we used for stock production resulted in purified stocks with titers of over 10^{11}/ml that were free of detectable RCV. Similar approaches to vector production should prove useful for other autonomous parvoviruses as well, allowing a variety of replication-incompetent vectors to be produced and their gene transfer potential to be assessed.

Our study is the first description of chromosomal integration by an autonomous parvoviral vector. Based on Southern blot analysis, integration occurred at random locations, and the vector proviruses had terminal deletions. Because the vector did not express NS1, this process is distinct from the NS1-dependent integration of MVM vectors into episomes (7, 8) and the related Rep-dependent site-specific integration of AAV vectors at human chromosome 19 (32, 49). Instead, MVM vector integration is similar to Rep-independent random integration of AAV vectors (38, 48, 53), which uses host enzymes in a reaction resembling nonhomologous end joining at double-strand breaks (36). Several lines of evidence suggest that single-stranded MVM vector genomes participated in the integration reaction. First, unlike AAV vectors, the MVM vectors delivered single strands of one polarity without complementary vector genomes. Second, these vectors did not undergo detectable second-strand synthesis to form double-stranded episomal molecules, although our analysis did not distinguish between unencapsidated vector genomes and those remaining in virions within the cell. Third, providing a mixture of forward and reverse vector stocks containing genomes that could have paired in vivo did not increase transduction frequencies. And fourth, providing NS1 protein and stimulating vector DNA replication by the addition of wild-type MVM did not increase integration frequencies. Thus, while we cannot completely rule out that rare double-stranded vector episomes were formed prior to integration, our evidence suggests that input single-stranded genomes ligated directly to chromosomal DNA (presumably at sites of DNA damage), and then subsequently completed second-strand synthesis. By analogy, the same single-strand integration process could occur with AAV vectors.

We also showed that autonomous parvovirus vectors can modify homologous chromosomal sequences in a gene-targeting reaction, similar to what we have described for AAV vectors (24, 46). Here again, our results suggest that the substrate for the gene-targeting reaction is the single-stranded input vector genome, supporting earlier data with AAV vectors showing that double-stranded self-complementary AAV vectors do not participate in gene targeting (25). In the *HPRT* experiments, forward orientation vector stocks that packaged the noncoding strand targeted more efficiently than reverse orientation vector stocks that packaged the coding strand. In contrast, the AP experiments had the opposite strand preference, with the reverse orientation, coding strand vector targeting at higher frequencies. The fact that one vector strand is superior to its complement is strong evidence for a single-stranded targeting substrate. In addition, since the strand preference was of opposite polarity in the AP and *HPRT* systems, the effect cannot be due to juxtaposition of the targeting sequence next to the nonidentical left- or right-terminal palindromes of MVM. Rather, it supports a model of gene targeting in which the target site determines which strand is better. This strand bias could be due to a number of cellular processes that make one chromosomal strand more accessible than the other, including DNA replication at leading and lagging strands, transcription, or DNA repair. Interestingly, there were a high proportion of random integration events in targeted cells transduced by the noncoding *HPRT* vector, raising the possibility that the inefficient targeting reaction taking place in these cells actually used the coding strand present at randomly integrated double-stranded proviruses.

While MVM vectors were able to transduce cells by random integration or gene targeting, AAV vectors were more efficient at both processes, even when used at lower MOIs. This is likely to be due at least in part to poor uptake of MVM in HT-1080 cells, since only 3.1% of input MVM vector genomes had entered cells 3 days after infection. Other cell types may be more permissive for MVM infection, and vectors based on different autonomous parvoviruses will likely have distinct host ranges, so there could still be applications in which autonomous parvoviral vectors are superior. Other factors could also explain the different transduction rates of AAV and MVM vectors, such as vector genome stability, effects of the different viral terminal repeats on the recruitment of host cell enzymes required for transduction, and possible intracellular reactions of the capsid proteins. Identification of these characteristics will improve our understanding of parvoviral transduction mechanisms and may lead to more effective clinical applications of these vectors.

ACKNOWLEDGMENTS

We thank Peter Tattersall for essential reagents; Daniel G. Miller for the cell line HT/AP375Δ4SP; and Rong Dong, Cong Xu, and Richard Newton for technical assistance.

This research was supported by grants from the National Institutes of Health.

REFERENCES

1. **Aitken, M. L., R. B. Moss, D. A. Waltz, M. E. Dovey, M. R. Tonelli, S. C. McNamara, R. L. Gibson, B. W. Ramsey, B. J. Carter, and T. C. Reynolds.** 2001. A phase I study of aerosolized administration of tgAAVCF to cystic fibrosis subjects with mild lung disease. Hum. Gene Ther. **12:**1907–1916.
2. **Avalosse, B. L., F. Dupont, P. Spegelaere, N. Mine, and A. Burny.** 1996. Method for concentrating and purifying recombinant autonomous parvovirus vectors designed for tumour-cell-targeted gene therapy. J. Virol. Methods **62:**179–183.
3. **Berns, K. I.** 1996. Parvoviridae: the viruses and their replication, p. 2173–2197. *In* B. N. Fields, D. M. Knipe, P. M. Howley et al. (ed.), Fields virology, 3rd ed. Lippincott-Raven Publishers, Philadelphia, Pa.
4. **Berns, K. I., and S. Adler.** 1972. Separation of two types of adeno-associated virus particles containing complementary polynucleotide chains. J. Virol. **9:**394–396.
5. **Bourguignon, G. J., P. J. Tattersall, and D. C. Ward.** 1976. DNA of minute virus of mice: self-priming, nonpermuted, single-stranded genome with a 5′-terminal hairpin duplex. J. Virol. **20:**290–306.
6. **Carter, P. J., and R. J. Samulski.** 2000. Adeno-associated viral vectors as gene delivery vehicles. Int. J. Mol. Med. **6:**17–27.
7. **Corsini, J., S. F. Cotmore, P. Tattersall, and E. Winocour.** 2001. The left-end and right-end origins of minute virus of mice DNA differ in their capacity to direct episomal amplification and integration in vivo. Virology **288:**154–163.
8. **Corsini, J., J. Tal, and E. Winocour.** 1997. Directed integration of minute virus of mice DNA into episomes. J. Virol. **71:**9008–9015.
9. **Cotmore, S. F., and P. Tattersall.** 1987. The autonomously replicating parvoviruses of vertebrates. Adv. Virus Res. **33:**91–174.
10. **Crawford, L. V., E. A. C. Follett, M. G. Burdon, and D. J. McGeoch.** 1968. The DNA of a minute virus of mice. J. Gen. Virol. **4:**37–46.
11. **DuBridge, R. B., P. Tang, H. C. Hsia, P.-M. Leong, J. H. Miller, and M. P. Calos.** 1987. Analysis of mutation in human cells by using an Epstein-Barr virus shuttle system. Mol. Cell. Biol. **7:**379–387.
12. **Dupont, F., B. L. Avalosse, A. Karim, N. Mine, M. Bosseler, A. Maron, A. V. Van den Broeke, G. E. Ghanem, A. Burny, and M. Zeicher.** 2000. Tumor-selective gene transduction and cell killing with an oncotropic autonomous parvovirus-based vector. Gene Ther. **7:**790–796.
13. **Dupont, F., A. Karim, J. C. Dumon, N. Mine, and B. L. Avalosse.** 2001. A novel MVMp-based vector system specifically designed to reduce the risk of replication-competent virus generation by homologous recombination. Gene Ther. **8:**921–929.
14. **Dupont, F., L. Tenenbaum, L.-P. Guo, P. Spegelaere, M. Zeicher, and J. Rommelaere.** 1994. Use of an autonomous parvovirus vector for selective transfer of a foreign gene into transformed human cells of different tissue origins and its expression therein. J. Virol. **68:**1397–1406.
15. **Ferrari, F. K., T. Samulski, T. Shenk, and R. J. Samulski.** 1996. Second-strand synthesis is a rate-limiting step for efficient transduction by recombinant adeno-associated virus vectors. J. Virol. **70:**3227–3234.
16. **Fields-Berry, S. C., A. L. Halliday, and C. L. Cepko.** 1992. A recombinant retrovirus encoding alkaline phosphatase confirms clonal boundary assignment in lineage analysis of murine retina. Proc. Natl. Acad. Sci. USA **89:**693–697.
17. **Fisher, K. J., G.-P. Gao, M. D. Weitzman, R. DeMatteo, J. F. Burda, and J. M. Wilson.** 1996. Transduction with recombinant adeno-associated virus for gene therapy is limited by leading-strand synthesis. J. Virol. **70:**520–532.
18. **Flotte, T., and B. Carter.** 1995. Adeno-associated virus vectors for gene therapy. Gene Ther. **2:**357–362.
19. **Gardiner, E. M., and P. Tattersall.** 1988. Mapping of the fibrotropic and lymphotropic host range determinants of the parvovirus minute virus of mice. J. Virol. **62:**2605–2613.
20. **Greelish, J. P., L. T. Su, E. B. Lankford, J. M. Burkman, H. Chen, S. K. Konig, I. M. Mercier, P. R. Desjardins, M. A. Mitchell, X. G. Zheng, J. Leferovich, G. P. Gao, R. J. Balice-Gordon, J. M. Wilson, and H. H. Stedman.** 1999. Stable restoration of the sarcoglycan complex in dystrophic muscle perfused with histamine and a recombinant adeno-associated viral vector. Nat. Med. **5:**439–443.
21. **Grimm, D., A. Kern, K. Rittner, and J. A. Kleinschmidt.** 1998. Novel tools for production and purification of recombinant adenoassociated virus vectors. Hum. Gene Ther. **9:**2745–2760.
22. **Haag, A., P. Menten, J. Van Damme, C. Dinsart, J. Rommelaere, and J. J. Cornelis.** 2000. Highly efficient transduction and expression of cytokine genes in human tumor cells by means of autonomous parvovirus vectors; generation of antitumor responses in recipient mice. Hum. Gene Ther. **11:**597–609.
23. **Henikoff, S., and M. K. Eghtedarzadeh.** 1987. Conserved arrangement of nested genes at the *Drosophila* Gart locus. Genetics **117:**711–725.
24. **Hirata, R., J. Chamberlain, R. Dong, and D. W. Russell.** 2002. Targeted transgene insertion into human chromosomes by adeno-associated virus vectors. Nat. Biotechnol. **20:**735–738.
25. **Hirata, R. K., and D. W. Russell.** 2000. Design and packaging of adeno-associated virus gene targeting vectors. J. Virol. **74:**4612–4620.
26. **Hirt, B.** 1967. Selective extraction of polyoma DNA from infected mouse cell cultures. J. Mol. Biol. **26:**365–369.
27. **Inoue, N., and D. W. Russell.** 1998. Packaging cells based on inducible gene amplification for the production of adeno-associated virus vectors. J. Virol. **72:**7024–7031.
28. **Josephson, N. C., G. Vassilopoulos, G. D. Trobridge, G. V. Priestley, B. L. Wood, T. Papayannopoulou, and D. W. Russell.** 2002. Transduction of human NOD/SCID-repopulating cells with both lymphoid and myeloid potential by foamy virus vectors. Proc. Natl. Acad. Sci. USA **99:**8295–8300.
29. **Kay, M. A., C. S. Manno, M. V. Ragni, P. J. Larson, L. B. Couto, A. McClelland, B. Glader, A. J. Chew, S. J. Tai, R. W. Herzog, V. Arruda, F. Johnson, C. Scallan, E. Skarsgard, A. W. Flake, and K. A. High.** 2000. Evidence for gene transfer and expression of factor IX in haemophilia B patients treated with an AAV vector. Nat. Genet. **24:**257–261.
30. **Kestler, J., B. Neeb, S. Struyf, J. Van Damme, S. F. Cotmore, A. D'Abramo, P. Tattersall, J. Rommelaere, C. Dinsart, and J. J. Cornelis.** 1999. *cis* requirements for the efficient production of recombinant DNA vectors based on autonomous parvoviruses. Hum. Gene Ther. **10:**1619–1632.
31. **Koeberl, D. D., I. E. Alexander, C. L. Halbert, D. W. Russell, and A. D. Miller.** 1997. Persistent expression of human clotting factor IX from mouse liver after intravenous injection of adeno-associated virus vectors. Proc. Natl. Acad. Sci. USA **94:**1426–1431.
32. **Kotin, R. M., R. M. Linden, and K. I. Berns.** 1992. Characterization of a preferred site on human chromosome 19q for integration of adeno-associated virus DNA by non-homologous recombination. EMBO J. **11:**5071–5078.
33. **Linden, R. M., E. Winocour, and K. I. Berns.** 1996. The recombination signals for adeno-associated virus site-specific integration. Proc. Natl. Acad. Sci. USA **93:**7966–7972.
34. **Maxwell, I. H., F. Maxwell, S. L. Rhode, J. Corsini, and J. O. Carlson.** 1993. Recombinant LuIII autonomous parvovirus as a transient transducing vector for human cells. Hum. Gene Ther. **4:**441–450.
35. **Merchlinsky, M. J., P. J. Tattersall, J. J. Leary, S. F. Cotmore, E. M. Gardiner, and D. C. Ward.** 1983. Construction of an infectious molecular clone of the autonomous parvovirus minute virus of mice. J. Virol. **47:**227–232.
36. **Miller, D. G., E. A. Rutledge, and D. W. Russell.** 2002. Chromosomal effects of adeno-associated virus vector integration. Nat. Genet. **30:**147–148.
37. **Moehler, M., B. Blechacz, N. Weiskopf, M. Zeidler, W. Stremmel, J. Rommelaere, P. R. Galle, and J. J. Cornelis.** 2001. Effective infection, apoptotic cell killing and gene transfer of human hepatoma cells but not primary hepatocytes by parvovirus H1 and derived vectors. Cancer Gene Ther. **8:**158–167.
38. **Nakai, H., Y. Iwaki, M. A. Kay, and L. B. Couto.** 1999. Isolation of recombinant adeno-associated virus vector-cellular DNA junctions from mouse liver. J. Virol. **73:**5438–5447.
39. **Nakai, H., E. Montini, S. Fuess, T. A. Storm, L. Meuse, M. Finegold, M. Grompe, and M. A. Kay.** 2003. Helper-independent and AAV-ITR-independent chromosomal integration of double-stranded linear DNA vectors in mice. Mol. Ther. **7:**101–111.
40. **Nakai, H., T. A. Storm, and M. A. Kay.** 2000. Recruitment of single-stranded recombinant adeno-associated virus vector genomes and intermolecular recombination are responsible for stable transduction of liver in vivo. J. Virol. **74:**9451–9463.
41. **Olijslagers, S., A. Y. Dege, C. Dinsart, M. Voorhoeve, J. Rommelaere, M. H. Noteborn, and J. J. Cornelis.** 2001. Potentiation of a recombinant oncolytic parvovirus by expression of apoptin. Cancer Gene Ther. **8:**958–965.
42. **Palmer, G. A., and P. Tattersall.** 2000. Autonomous parvoviruses as gene transfer vehicles. Contrib. Microbiol. **4:**178–202.
43. **Rasheed, S., W. Nelson-Rees, E. Toth, P. Arnstein, and M. Gardner.** 1974. Characterization of a newly derived human sarcoma cell line (HT-1080). Cancer **33:**1027–1033.
44. **Richards, R. G., and R. W. Armentrout.** 1979. Early events in parvovirus replication: lack of integration by minute virus of mice into host cell DNA. J. Virol. **30:**397–399.
45. **Ron, D., and J. Tal.** 1985. Coevolution of cells and virus as a mechanism for the persistence of lymphotropic minute virus of mice in L-cells. J. Virol. **55:**424–430.
46. **Russell, D. W., and R. K. Hirata.** 1998. Human gene targeting by viral vectors. Nat. Genet. **18:**325–330.
47. **Russell, D. W., and M. A. Kay.** 1999. Adeno-associated virus vectors and hematology. Blood **94:**864–874.
48. **Rutledge, E. A., and D. W. Russell.** 1997. Adeno-associated virus vector integration junctions. J. Virol. **71:**8429–8436.
49. **Samulski, R. J., X. Zhu, X. Xiao, J. D. Brook, D. E. Housman, N. Epstein,**

and L. A. Hunter. 1991. Targeted integration of adeno-associated virus (AAV) into human chromosome 19. EMBO J. **10:**3941–3950.

50. **Tam, P., and C. R. Astell.** 1993. Replication of minute virus of mice minigenomes: novel replication elements required for MVM DNA replication. Virology **193:**812–824.
51. **Tattersall, P., and J. Bratton.** 1983. Reciprocal productive and restrictive virus-cell interactions of immunosuppressive and prototype strains of minute virus of mice. J. Virol. **46:**944–955.
52. **Weitzman, M. D., S. R. Kyostio, R. M. Kotin, and R. A. Owens.** 1994. Adeno-associated virus (AAV) Rep proteins mediate complex formation between AAV DNA and its integration site in human DNA. Proc. Natl. Acad. Sci. USA **91:**5808–5812.
53. **Yang, C. C., X. Xiao, X. Zhu, D. C. Ansardi, N. D. Epstein, M. R. Frey, A. G. Matera, and R. J. Samulski.** 1997. Cellular recombination pathways and viral terminal repeat hairpin structures are sufficient for adeno-associated virus integration in vivo and in vitro. J. Virol. **71:**9231–9247.